Light localization induced by a random imaginary refractive index

A. Basiri,[1] Y. Bromberg,[2] A. Yamilov,[3] H. Cao,[2] and T. Kottos[1]
[1]*Department of Physics, Wesleyan University, Middletown, Connecticut 06459, USA*
[2]*Department of Applied Physics, Yale University, New Haven, Connecticut 06520, USA*
[3]*Department of Physics, Missouri University of Science and Technology, Rolla, Missouri 65409, USA*
(Received 23 February 2014; revised manuscript received 14 May 2014; published 13 October 2014)

We show the emergence of light localization in arrays of coupled optical waveguides with randomness only in the imaginary part of their refractive index and develop a one-parameter scaling theory for the normalized participation number of Floquet-Bloch modes. This localization introduces a different length scale in the decay of the autocorrelation function of a paraxial beam propagation. Our results are relevant to a vast family of systems with randomness in the dissipative part of their impedance spatial profile.

DOI: 10.1103/PhysRevA.90.043815 PACS number(s): 42.25.Dd, 05.60.−k, 42.25.Bs, 72.15.Rn

I. INTRODUCTION

Wave propagation in random media is of great fundamental and applied interest. It covers areas ranging from quantum physics and electromagnetic wave propagation to acoustics and atomic-matter wave systems. Despite this diversity, the underlying wave character of these systems provides a unified framework for understanding mesoscopic transport and often points to new applications. A celebrated example of this universal behavior of wave propagation is the so-called Anderson localization phenomenon associated with a halt of transport in a random medium due to interference effects originating from multiple-scattering events [1]. In recent years, a number of experiments with classical [2–10] and matter waves [11,12] have confirmed the validity of this prediction. In all these cases, however, the wave localization originates from randomness pertaining to the spatial profile of the reactive part of the impedance.

In the present paper we show the emergence of localization phenomena in a different setting, namely a class of systems, whose the spatial impedance profile has random dissipative part. Realizations of this class can include Bose-Einstein condensates in randomly leaking optical lattices, acoustic or electromagnetic wave propagation in a medium with random losses, and even quantum random-walk protocols in the presence of traps that are used in the context of quantum computation.

For concreteness, we will refer below to a representative example of this class of systems drawn from optics: an array of N coupled waveguides with complex index of refraction $\epsilon_n = \epsilon_n^{(R)} + i\epsilon_n^{(I)}$ where the real part $\epsilon_n^{(R)}$ can be the same for all waveguides while their imaginary part $\epsilon_n^{(I)}$ is a random independent variable given by some distribution. We find that the Floquet-Bloch (FB) modes $\Phi^{(\omega)} = (\phi_1^{(\omega)}, \ldots, \phi_n^{(\omega)}, \ldots)^T$ ($\phi_n^{(\omega)}$ is the amplitude of the FB mode at waveguide $n = 1, \ldots, N$ associated with an eigenfrequency ω) are exponentially localized with localization centers being waveguides with positive or negative imaginary refractive index alike. We show that the participation number $\xi_N(W,\omega) \equiv (\sum_n |\phi_n|^2)^2 / \sum_n |\phi_n|^4$ of the FB modes obeys an one-parameter scaling:

$$\frac{\partial p_N(W,\omega)}{\partial \ln N} = \beta(p_N(W,\omega)); \quad p_N(W,\omega) \equiv \frac{\langle \xi_N(W,\omega)\rangle}{N}. \quad (1)$$

Above β is a *universal* function of $p_N(W,\omega)$ alone, which is independent of any microscopic properties of the system, and $\langle \xi_N(W,\omega)\rangle \equiv 1/\langle \sum_n |\phi_n|^4 / (\sum_n |\phi_n|^2)^2 \rangle$ denotes an averaging over FB modes within a small frequency window and over disorder realizations. The variable W defines the disorder strength associated with $\epsilon_n^{(I)}$ and it introduces a new length scale $\xi_\infty \equiv \lim_{N\to\infty} \xi_N$ which is inversely proportional to the asymptotic decay rate of the FB modes. The transverse localization of the FB modes plays an important role in the beam propagation. Specifically we find that the normalized autocorrelation function $C(z) \equiv (1/z) \int_0^z (|\psi_{n_0}(z')|^2 dz') / \sum_n |\psi_n(z)|^2$ of a propagating beam $\psi_n(z)$ which is initially localized at waveguide n_0 deviates from its periodic lattice analog at propagation distances $z^* \sim \sqrt{\xi_\infty / \Delta[\mathrm{Im}(\omega)]}$ where $\Delta[\mathrm{Im}(\omega)]$ is the spread of the eigenfrequencies in the complex plane. Our results are not affected by the sign of the random variable $\epsilon_n^{(I)}$ thus unveiling a duality between gain ($\epsilon_n^{(I)} < 0$) and lossy ($\epsilon_n^{(I)} > 0$) structures.

We point out that the effect of imaginary index of refraction on Anderson localization of light has been studied by a number of authors [13–15]. In all these cases, however, the authors were considering light localization along the propagation direction and their conclusions were based on the solutions obtained from the time-independent Schrödinger or Maxwell's equation. One of the main findings was that both gain and loss lead to the same degree of suppression of transmittance [13,14]. This counterintuitive duality was shown in Ref. [15], using time-dependent Maxwell's equation, to be an artifact of time-independent calculations. Specifically, it was shown that the amplitudes of both transmitted and reflected waves diverge due to lasing (in the case of gain) above a critical length scale. In contrast, in our setup where localization is transverse to the paraxial propagation, divergence would not occur at any finite propagation distance and therefore the solutions of our problem are physically realizable.

II. PHYSICAL SETUP

We consider a one-dimensional array of weakly coupled single-mode optical waveguides. The light propagation along the z axis is described by the equations [16]

$$i\lambda \frac{\partial \psi_n(z)}{\partial z} + V[\psi_{n+1}(z) + \psi_{n-1}(z)] + \epsilon_n \psi_n(z) = 0, \quad (2)$$

where $n = 1, \ldots, N$ is the waveguide number, $\psi_n(z)$ is the amplitude of the optical field envelope at distance z in the nth waveguide, $\lambda \equiv \lambda/2\pi$ where λ is the optical wavelength, and V is the tunneling constant between nearby waveguides. In order to identify and isolate localization phenomena due to the randomness of the imaginary index of refraction, we have assumed that V is real and constant for all waveguides. Below for simplicity we consider that $V = 1$. Nevertheless, one needs to point out that this approximation has limitations (see for example [17]) as the coupling coefficient depends on the refractive index of the waveguides. Furthermore in cases or random imaginary indices of refraction the coupling coefficients can have a small imaginary component [18,19]. Finally $\epsilon_n = \epsilon_n^{(R)} + i\epsilon_n^{(I)}$ is the complex on-site effective index of refraction. Optical amplification can be introduced by stimulated emission in gain material or parametric conversion in nonlinear material [20], whereas dissipation can be incorporated by depositing a thin film of absorbing material on top of the waveguide [18], or by introducing scattering loss in the waveguides [19]. In order to distinguish the well understood Anderson localization phenomena which are associated with random $\epsilon_n^{(R)}$ from the localization phenomena related to the randomness of the imaginary part $\epsilon_n^{(I)}$, we consider below that all the waveguides have an identical effective index $\epsilon_n^{(R)} = \epsilon_0$ while $\epsilon_n^{(I)}$ is a random variable uniformly distributed in an interval $[-W; W]$. Due to the Kramers-Kronig relations the real and imaginary part of the dielectric constant are not independent of each other, nevertheless it is possible to have disorder only in the imaginary part by compensating for the changes in the $\epsilon_n^{(R)}$ by adjusting, for example, the width of the waveguides. The advantage offered by our system is the ability to study the dynamics of synthesized wave packets, by launching an optical beam into any one waveguide or a superposition of any set of waveguides, and monitoring from the third dimension.

Substituting $\psi_n(z) = \phi_n \exp(-i\omega z)$, where ω can be complex, in Eq. (2) we get the eigenvalue problem

$$\omega\phi_n = -(\phi_{n+1} + \phi_{n-1}) - \epsilon_n\phi_n. \tag{3}$$

We note that the spectral properties of this type of equations have been investigated thoroughly in the mathematical physics literature [21–23].

In Fig. 1(a) we report some typical FB modes for one realization of the disorder. Even though the disorder is only in the imaginary part of the index of refraction, for sufficiently large disorder (or large system size) all modes are exponentially localized around a center which can be either a gain (red) or a lossy (green) waveguide alike. To reveal the localization mechanism, we plot in Fig. 1(b) the phase profiles of the localized modes with the maximum and the minimum imaginary component of ω respectively. The former is localized around a waveguide with gain, and has a "V" shaped phase profile, indicating an energy flow away from the center of the mode. Thus the optical diffraction is balanced by preferable amplification in the central waveguide, keeping the localized mode profile invariant with propagation (the magnitude increases). The other mode is localized on a waveguide with loss, and its phase profile has a "Λ" shape, corresponding to an energy flow towards the center of the mode. The reduction in the field amplitude at the central

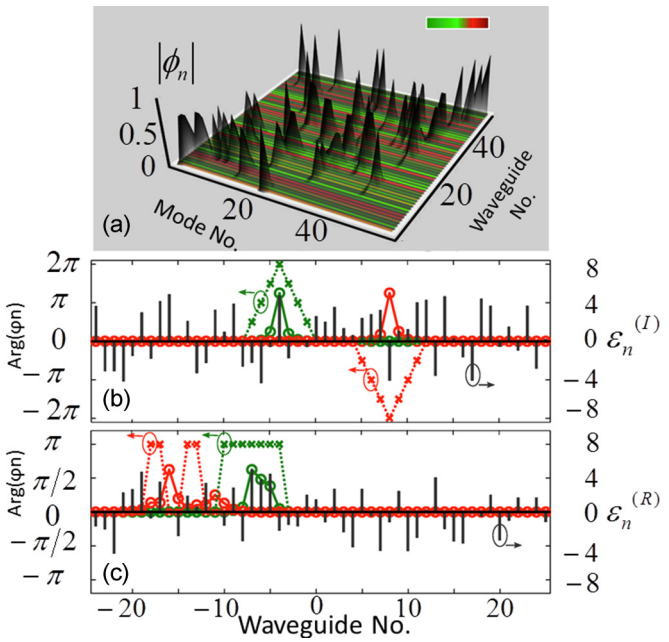

FIG. 1. (Color online) (a) The normalized Floquet-Bloch modes of an array of $N = 50$ waveguides with random imaginary index of refraction taken from a box distribution with width $W = 5$. All modes are exponentially localized at various localization centers corresponding to gain (red stripes) (or dark gray stripes in grayscale version) or loss (green stripes) (or bright stripes in grayscale version) waveguides alike. (b) Amplitude (solid line, open circles) and phase (dashed line, crosses) of a mode localized around a center corresponding to gain (red, right) or loss (green, left). The phase profile of the gain (loss) mode corresponds to a wave diverging from (converging towards) the center of the localized mode. The left axis corresponds to the phase profile. The bars indicate the imaginary value of the index of refraction $\epsilon_n^{(I)}$ (right axis). (c) Same as (b) for the Anderson model with disorder only in the real part of the refractive index. The bars correspond to $\epsilon_n^{(R)}$. The green (red) mode is at the top (center) of the band, and its phase profile is flat (jumping between 0 and π every two waveguides).

waveguide due to absorption and diffraction is overcome by the continuous supply of energy from neighboring waveguides via the "focusing" effect. Typically a focused beam would diverge after the focal spot, but in this case the outgoing wave is completely absorbed by the central waveguide, so the mode remains localized along the propagation direction. Such localization mechanism, which bears similarity to gain and loss guiding in continuous media [24], is qualitatively different from the Anderson model with disorder only in the real part of the index of refraction, where the localization is a result of interference of multiply scattered light. In the Anderson model the phase profile of the localized modes is set by the position of the mode inside the band, e.g., modes at the top of the band have a flat phase and modes at the center of the band exhibit a π-phase flip typically every other cite [Fig. 1(c)].

The same qualitative picture applies also for the cases where all $\epsilon_n^{(I)}$ are positive (and random) or negative (and random). Therefore, our setup supports a *duality* between gain and loss. We want to quantify the structure of the FB modes of

our system and identify the consequences of their transverse localization to the spreading.

III. EXPONENTIAL LOCALIZATION IN THE THERMODYNAMIC LIMIT

We start our analysis by introducing the asymptotic participation number ξ_∞ defined as

$$\xi_\infty(W) = \lim_{N\to\infty} \langle \xi_N(W) \rangle \equiv \lim_{N\to\infty} \left\langle \sum_n |\phi_n|^4 \Big/ \left(\sum_n |\phi_n|^2 \right)^2 \right\rangle^{-1}. \quad (4)$$

Above the averaging has been performed over a number of disorder realizations and over FB modes inside a small frequency window around a fixed $\mathrm{Re}(\omega)$. In all cases we had at least 8000 data for statistical processing.

In Fig. 2(a) we report some representative data for the participation number $\langle \xi_N \rangle$, as a function of the system size N for various disorder strengths W and for $\mathrm{Re}(\omega) = 0$. The same analysis applies for other values of ω as well. From the data of Fig. 2(a) we have extracted the saturation value $\xi_\infty(W,\omega)$. The results are summarized in Fig. 2(b) where we plot $\xi_\infty(W,\omega)$, associated for the specific $\mathrm{Re}(\omega) = 0$ (band center), vs W. Our analysis indicates that $\xi_\infty \sim 1/W^2$. In case of exponentially localized FB modes, it is easy to show that $\xi_\infty(W,\omega)$ is proportional to the inverse decay rate $\gamma(W,\omega)$ [see Eq. (5) below] of these modes.

We shall now derive an explicit expression for the decay rate $\gamma(\omega)$ associated with a normal mode of specific frequency ω. In order to obtain the transverse exponential growth (or decay) of the wave-function amplitudes ϕ_n at sites n we solve Eq. (3) recursively starting from some arbitrary value ϕ_{n_0}, at site n_0. We define

$$\gamma \equiv -\lim_{N\to\infty} \frac{1}{N} \left\langle \ln \left| \frac{\phi_N}{\phi_{n_0}} \right| \right\rangle = -\lim_{N\to\infty} \frac{1}{N} \left\langle \sum_{n_0}^{N} \ln |R_n| \right\rangle, \quad (5)$$

where we have introduced the so-called Riccati variable $R_n \equiv \frac{\phi_n}{\phi_{n-1}}$. We can rewrite Eq. (3) as follows:

$$R_{n+1} + \frac{1}{R_n} = (\omega - \epsilon_n), \quad (6)$$

where now ω is considered an arbitrary frequency which we use as an input parameter [25]. Using Eqs. (5) and (6) we can then evaluate numerically $\gamma(W,\omega)$.

Next we write R_n as $A \times \exp(W B_n + W^2 C_n + \cdots)$ and substitute in Eq. (6) $\omega = 2\cos q$, where q is in general a complex quantity. For weak disorder we can further expand R_n in Taylor series of W. Equating the same powers of W in Eq. (6) while taking into consideration the statistical nature of ϵ_n (e.g., $\langle \epsilon_n \rangle = 0$), we get expressions for A, $\langle B_n \rangle$, $\langle B_n^2 \rangle$, and $\langle C_n \rangle$ as a function of W. Substituting them back to Eqs. (5) and (6) we get, up to second order in W, that

$$\gamma = q_I + \left(\frac{W^2}{24} \right) \times \frac{\omega_I^2 \coth^2(q_I) - \omega_R^2 \tanh^2(q_I)}{\left(\frac{1}{4}\right)\left[\omega_I^2 \coth^2(q_I) - \omega_R^2 \tanh^2(q_I)\right]^2 + \omega_I^2 \omega_R^2}, \quad (7)$$

where $\omega_R = \mathrm{Re}(\omega); \omega_I = \mathrm{Im}(\omega); q_R = \mathrm{Re}(q); q_I = \mathrm{Im}(q)$. A comparison between the theoretical expression Eq. (7) and the numerically extracted asymptotic participation number ξ_∞ is shown in Fig. 2(b). Finally, we point that the above analysis does not take into consideration anomalies in the localization length associated with the band edge of the spectrum. Such type of anomalies are known to exist for the case of real disorder and can lead to a different scaling of the localization length with the disorder strength W [27].

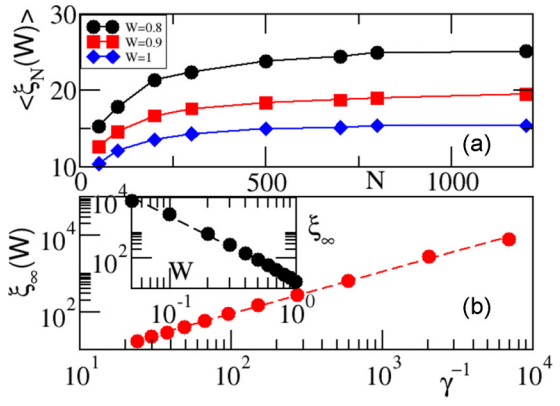

FIG. 2. (Color online) (a) The participation number $\langle \xi_N(W) \rangle$ (in units of lattice spacing) vs the system size N (in units of lattice spacing) for various disorder strengths W. A small energy window around $\mathrm{Re}(\omega) = 0$ such that $\mathrm{Re}(\omega) \in [-0.1, 0.1]$ has been considered. (b) The extracted asymptotic participation number vs the prediction of Eq. (7) for the exponential decay rate γ. The best-squares fit (dashed line) gives $\xi_\infty = 0.55\gamma^{-1}$. In the inset we report the $\xi_\infty(W)$ (in units of lattice spacing) vs W for a specific frequency window around $\mathrm{Re}(\omega) = 0$. The best-squares fit (dashed line) is $\xi_\infty(W) \sim W^{-2}$.

IV. ONE-PARAMETER SCALING THEORY

We are now ready to formulate a one-parameter scaling theory of the finite length participation number of the FB modes of our system Eq. (3). To this end we postulate the existence of a function $f(\Lambda)$ such that

$$p_N(W) = f(\Lambda) \quad \text{where} \quad \Lambda \equiv \frac{\xi_\infty}{N}, \quad (8)$$

where $p_N(W)$ is defined in Eq. (1). In the localized regime $\Lambda \ll 1$ (infinite system sizes N) the participation number $\xi_N(W,\omega)$ has to converge to its asymptotic value $\xi_\infty(W,\omega)$ [see Eq. (4)] thus we expect that $f(\Lambda) \to \Lambda$. In the other limiting case $\Lambda \gg 1$, corresponding to the delocalized regime, we have that $\xi_N(W) \propto 2N/3$ and thus $f(\Lambda) \to 2/3$ [28].

We have confirmed numerically the validity of Eq. (8) for our system; see Fig. 3. Various values of N in the range 100–1200 have been used while the width of the box distribution W was taken at $0.05 \leqslant W \leqslant 1$. We have also checked (not shown here) that the same scaling behavior is applicable for the case where n_I takes random values which are only positive or negative.

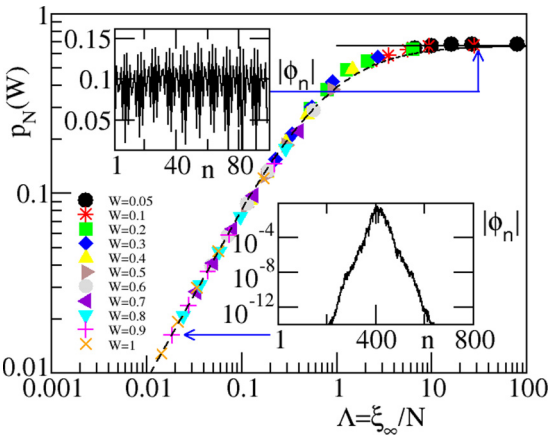

FIG. 3. (Color online) Scaled participation ratio $p_N(W) \equiv \xi_N/N$ vs the scaling parameter $\Lambda \equiv \xi_\infty/N$ for various N values and disorder strengths $W = 0.1$–1. The eigenmodes are taken from a small frequency window at the center of the band. Insets: Two typical FB modes in the localized (lower left) and in the delocalized (upper right) domain. The arrows indicate the corresponding values of the localization parameter Λ. The solid line is the theoretical value of 2/3 for the limiting case of $\Lambda \gg 1$. For comparison we also report (dashed black line) the results of the standard Anderson model [Eq. (9) with $D \approx 1.4$] with real random on-site potential taken in the interval $[-W; W]$.

It is then straightforward to show that Eq. (8) can be written equivalently in the form of Eq. (1). Indeed, taking the derivative of Eq. (8) with respect to $\ln(N)$ we get that $\partial p_N(W)/\partial \ln N = -\Lambda \partial f(\Lambda)/\partial \Lambda = F(\Lambda)$. Substituting $\Lambda = f^{-1}(p_N(W))$ back to the latter equation allows us to rewrite the right-hand side of it as $F(\Lambda = f^{-1}(p_N(W))) = \beta(p_N(W))$ which proves the validity of Eq. (1).

For comparison we have also plotted in Fig. 3 the theoretical results for the scaled participation number for the equivalent case of the standard Anderson model with real random refractive indexes $\epsilon_n \in [-W; W]$. The scaling properties of the participation number, in this case, have been investigated in a number of papers [29,30]. Specifically these authors have found that the scaled participation number is described by a universal law:

$$p_N = \frac{2}{3}\frac{D\Lambda}{1+D\Lambda} \leftrightarrow \frac{1}{\xi_N} = \frac{1}{\xi_{\text{ref}}} + \frac{1}{\xi_\infty}, \tag{9}$$

where D is a model-dependent constant, and ξ_{ref} is the participation number of an underlying reference system associated to maximally ergodic eigenstates (in our case this is the perfect lattice with $\xi_{\text{ref}} = 2N/3$). The validity of this expression has been tested in a variety of disordered models [31].

We find that our results for the scaled participation number in the case of random imaginary refractive indexes follow nicely the results of the standard Anderson case. This striking similarity indicates that as far as the participation number is concerned, localization phenomena are insensitive to the origin of impedance mismatch that leads to them.

V. TEMPORAL CORRELATIONS AND BREAK TIME

A natural question is how is the transverse localization of the Floquet-Bloch modes reflected in the paraxial propagation of a beam which is initially localized at some waveguide n_0. A dynamical observable that can be used in order to trace the effects of localization is the return to the origin probability $P_{n_0}(z) = |\psi_{n_0}(z)|^2 \equiv |\langle n_0|\psi(z)\rangle|^2$. For lossless random media $P_{n_0}(z \to \infty) \sim \xi_\infty^{-1}$. In contrast, for periodic lattices $P_{n_0}(z) = |J_0(2Vz)|^2$ where $J_0(x)$ is the zeroth-order Bessel function. Since $P_{n_0}(z)$ is a fluctuating quantity, we often investigate its smoothed version $C(z) = (1/z)\int_0^z P(z')dz'$. For periodic lattices $C(z) \sim 1/z$, indicating a loss of correlations of the evolving beam with the initial preparation.

We have introduced a rescaled version of $\tilde{C}(z)$ such that it takes into account the growth or loss of the total field intensity due to the presence of the dissipative part of the index of refraction at the waveguides

$$\tilde{C}(z) = \frac{1}{z}\int_0^z P(z')dz'/I(z), \quad I(z) = \sum_n |\psi_n(z)|^2 \tag{10}$$

and compare its deviations from the ballistic results $\tilde{C}_{\text{bal}}(z) \sim 1/z$ corresponding to a perfect lattice [32]. We have found that the correlation function of the disordered lattice follows the ballistic results up to a propagation distance z^* which depends on the disorder W of $n^{(I)}$. We determined the break length z^* by the condition $Q(z) = [\tilde{C}(z)/\tilde{C}_{\text{bal}}(z)] - 1 = 0.1$ which corresponds to 10% deviations of $\tilde{C}(z)$ from the behavior shown by the perfect lattice. To suppress the ensemble fluctuations further, we averaged $\tilde{C}(z)$ over more than 50 different disorder realizations. Then the (averaged) break length z^* is determined by the condition $\langle Q(z^*)\rangle = 0.1$. The dependence of $\langle Q(z)\rangle$ on distance, for representative disorder widths W, is shown in Fig. 4(a). We find that z^* becomes smaller as we increase the disorder W. The numerically extracted z^* values and their dependence on W are summarized in Fig. 4(b). The fit of the numerical data gives a power-law

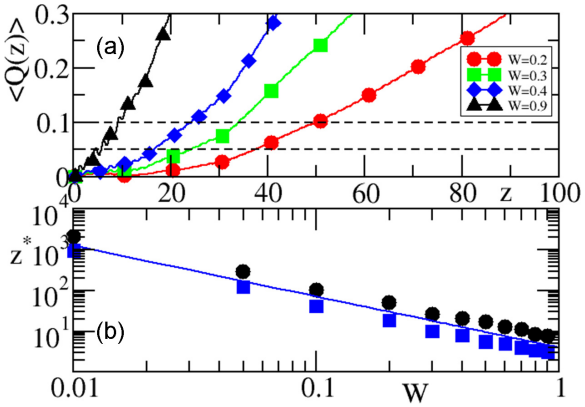

FIG. 4. (Color online) (a) The averaged $\langle Q(z)\rangle$ vs distance z (units of λ/V) for typical values of disorder strength W. The horizontal black dashed lines indicate a 5% (lower) and 10% (upper) deviation of $\tilde{C}(z)$ from the ballistic result $\tilde{C}_{\text{bal}}(z)$. (b) The break length z^* (in units of λ/V) vs W for 5% (blue squares) and 10% (black circles) deviations. The straight line is the best fit and has a slope −1.4.

dependence $z^* \approx W^{-\alpha}$ with $\alpha \approx 1.4$, being quite robust to other definitions (e.g., 5% deviation level) of break length.

The following heuristic argument provides some understanding of the dependence of the break length on the disorder strength. Our explanation is based on the fact that in a non-Hermitian system the physics is affected by the distribution of the complex frequencies of the effective non-Hermitian Hamiltonian that describes the paraxial evolution of the beam in the waveguide array.

Once the disorder W is introduced to the imaginary part of the refractive indexes, the eigenfrequencies acquire an imaginary part that determines the growth or decay of the associated normal modes of the system. They are distributed in an area $\mathcal{A}$ in the complex plane around the real axis. In Ref. [21] the density of complex eigenmodes $\rho(\mathrm{Re}(\omega),\mathrm{Im}(\omega))$ has been calculated in the case of weak disorder in the self-consistent Born approximation (mean field) and it was found to be

$$\rho(\mathrm{Re}(\omega),\mathrm{Im}(\omega)) = \begin{Bmatrix} \left(4\pi\sigma_W^2\right)^{-1} & |\mathrm{Im}(\omega)| < \Delta\mathrm{Im}(\omega) \\ 0 & |\mathrm{Im}(\omega)| > \Delta\mathrm{Im}(\omega) \end{Bmatrix}, \tag{11}$$

where $\Delta\mathrm{Im}(\omega) = 2\sigma_W^2/\sqrt{4V^2 - \mathrm{Re}(\omega)^2}$ and σ_W^2 is the variance of the imaginary random potential (in the case of box distribution $[-W,W]$ we get that $\sigma_W^2 = W^2/3$). Although Eq. (11) applies for values of $\mathrm{Re}(\omega)$ such that $\mathrm{Re}(\omega) \gg \Delta\mathrm{Im}(\omega)$, nevertheless, it captures nicely the envelope of the distribution of complex eigenmodes. In Fig. 5(a) we depicted a typical distribution of eigenvalues of our non-Hermitian Hamiltonian. Notice that modes at the edges of the band move further up or down in the complex plain, as predicted by Eq. (11) [21]. At the same time some modes are outside of the envelope indicating the existence of rare states associated with anomalously strong fluctuations of the imaginary potential (Lifshitz-like states) [21].

We have also evaluated numerically the variance $\sigma^2_{\mathrm{Im}(\omega)}$ of the imaginary part of the complex frequencies of the non-Hermitian Hamiltonian (3). In Fig. 5(b), the scaling of the standard deviation $\sigma_{\mathrm{Im}(\omega)} \propto \Delta\mathrm{Im}(\omega)$ is presented vs the disorder amplitude W. We find the following scaling relation:

$$\sigma_{\mathrm{Im}(\omega)} \sim W^{1.6} \tag{12}$$

which is close to the theoretical prediction of Eq. (11). We attribute the difference to the fact that the theoretical prediction has limitations, namely it does not consider the possibility of rare states existing outside the envelope $\Delta\mathrm{Im}(\omega)$.

One can further approximate the area $\mathcal{A}$ at which the complex eigenmodes are distributed as $\mathcal{A} \sim \Delta\mathrm{Re}(\omega) \cdot \Delta\mathrm{Im}(\omega)$. The length of the area is fixed $\Delta\mathrm{Re}(\omega) \propto 2V$ while its width $\Delta\mathrm{Im}(\omega)$ is given by Eq. (11) as $\Delta\mathrm{Im}_{\mathrm{Th}}(\omega) \propto W^2$ or if we take into consideration the rare events by the numerical value of Eq. (12) $\Delta\mathrm{Im}_{\mathrm{Num}}(\omega) \propto W^{1.6}$. Accordingly we have that $\mathcal{A}_{\mathrm{Th}} \sim W^2$ and $\mathcal{A}_{\mathrm{Num}} \sim W^{1.6}$.

Since, on the other hand, the FB modes are localized then only ξ_∞ out of them have a significant overlap with the initial localized state and thus effectively participate in the evolution. Their effective frequency spacing in the complex plane δ defines the energy scale that determines the deviations from periodic lattice behavior. The associated break length is defined as $z^* \sim 1/\delta$. The latter is estimated by realizing that $\xi_\infty \delta^2 \approx \mathcal{A}$. Solving with respect to δ we get

$$\begin{aligned} \delta_{\mathrm{Th}} &\sim \sqrt{\mathcal{A}_{\mathrm{Th}}/\xi_\infty} \sim W^2 \rightarrow z^* \sim 1/\delta \sim W^{-2}, \\ \delta_{\mathrm{Num}} &\sim \sqrt{\mathcal{A}_{\mathrm{Num}}/\xi_\infty} \sim W^{1.8} \rightarrow z^* \sim 1/\delta \sim W^{-1.8}. \end{aligned} \tag{13}$$

The prediction of Eq. 13(b) agrees better to the numerical value 1.4 that we got from the best-squares fit in Fig. 4. The difference is attributed to the fact that the localization length used in Eq. (13) is associated with the modes around $\mathrm{Re}(\omega) \approx 0$ while for other frequencies (e.g., closer to the band edges of the real axis) it might scale as $\xi_\infty \sim 1/W^\mu$ with $\mu < 2$ (Wegner-Kappus anomalies). To incorporate for the fact that an initial δ-like beam excites FB modes with various frequencies, in the next section we introduce an *average localization length over all frequencies*.

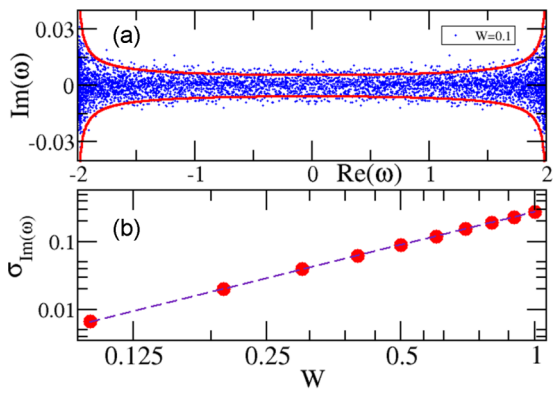

FIG. 5. (Color online) (a) Imaginary vs real parts of eigenvalues for $N = 500$ and $W = 0.1$. The red line indicates the envelope of the area for which the complex eigenmodes are distributed [see Eq. (11)]. (b) The standard deviation of $\mathrm{Im}(\omega)$ as a function of W. The least-squares fit (dashed line) indicates $\sigma_{\mathrm{Im}(\omega)} \sim W^{1.6}$.

VI. SCALING QUANTITIES AFTER AVERAGING OVER THE WHOLE SPECTRUM

In this section we study the scaling of localization length $\bar{\xi}_\infty$ vs the disordered strength W when the averaging over the eigenmodes of the effective Hamiltonian Eq. (3) is performed over the whole frequency spectrum. Our starting point is the definition in Eq. (4):

$$\begin{aligned} \bar{\xi}_\infty(W) &= \lim_{N\to\infty} \langle \overline{\xi_N(W)} \rangle \\ &\equiv \lim_{N\to\infty} \left\langle \sum_n |\phi_n|^4 \Big/ \left(\sum_n |\phi_n|^2 \right)^2 \right\rangle^{-1}, \end{aligned} \tag{14}$$

where $\langle \cdots \rangle$ indicates the standard averaging over disorder realizations as defined in the Introduction and $\overline{\cdots}$ is the additional averaging over the whole frequency spectrum. Some representative data for the finite participation number $\bar{\xi}_N(W)$ vs the system size N are shown in Fig. 6(a). A summary of the extracted asymptotic values $\bar{\xi}_\infty(W)$ is shown in Fig. 6(b). The least-squares fit indicates that

$$\bar{\xi}_\infty(W) \sim W^{-1.27}. \tag{15}$$

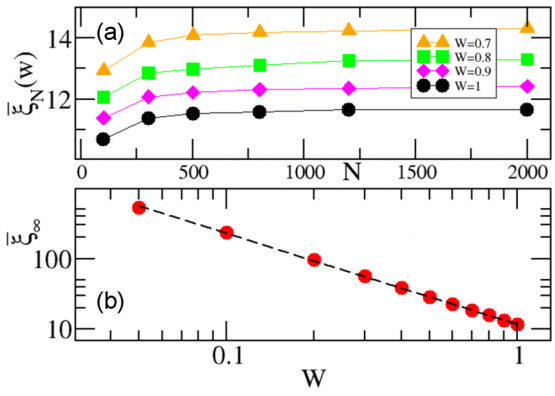

FIG. 6. (Color online) (a) Asymptotic behavior of the participation number $\bar{\xi}_N(W)$ (units of lattice spacing) for the large system sizes N (units of lattice spacing) and various disorder strengths W. These data cover the whole energy window where $\mathrm{Re}(\omega) \in [-2,2]$. (b) Asymptotic participation number $\bar{\xi}_\infty(W)$ vs the disorder strength W follows a scaling as $\bar{\xi}_\infty(W) \sim W^{-\mu}$ with $\mu = 1.27$ given by the least-squares fit.

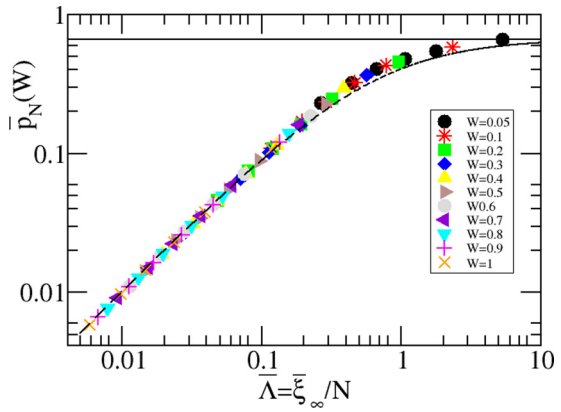

FIG. 7. (Color online) Scaled participation ratio $\bar{p}_N(W) \equiv \bar{\xi}_N/N$ vs the scaling parameter $\bar{\Lambda} \equiv \bar{\xi}_\infty/N$ for various N's and disorder strengths $W = 0.05$–1. The eigenmodes belong to whole frequency range. The theoretical value of $2/3$ (black line) is confirmed for the limiting case of $\Lambda \gg 1$. The black dashed line is the theoretical prediction Eq. (9) for the corresponding standard Anderson model with disorder in the real part of the index of refraction and $D \approx 1.55$. An averaging over the whole spectrum is considered.

We have also confirmed the validity of Eq. (15) by establishing that it is the appropriate variable for the applicability of the one-parameter scaling theory of the participation number in the case where the averaging is performed over the whole spectrum. The associated rescaled participation number $\bar{p}_N(W) \equiv \bar{\xi}_N/N$ vs the scaling parameter $\bar{\Lambda} \equiv \bar{\xi}_\infty(W)/N$ is reported in Fig. 7. We point out here that the applicability of the scaling law Eq. (8) is guaranteed also for the spectral averaged quantities, if one assumes the validity of Eq. (9) as well. The latter equation can be rewritten in the form $\overline{\langle \sum_n |\phi_n|^4 / (\sum_n |\phi_n|^2)^2 \rangle} = 3/2N + 1/\bar{\xi}_\infty$. A nice scaling is evident.

Armed with the above knowledge of Eq. (15) we apply the argument of Eq. 13(b) and re-evaluate the prediction of break time z^*, under the (more realistic) assumption that all modes participate in the evolution of the wave packet. Substituting Eqs. (12) and (15) in Eq. 13(b) we find that $z^* \sim W^{-1.435}$ which is within the numerical accuracy of our extracted value of $\alpha = 1.4$ from the numerical analysis of Fig. 4.

VII. CONCLUSIONS

In conclusion, we have demonstrated that randomness only in the dissipative part of the impedance profile of a medium can result in localization. By analyzing the localized FB modes in an array of coupled waveguides with random gain and loss as a prototype for this class of systems, we found that the physical mechanism of the localization in this system is qualitatively different from the localization mechanism of Anderson localization. Nevertheless, the scaling behavior of the two systems is similar. We found that the participation number of the FB modes of the effective non-Hermitian Hamiltonian exhibits a one-parameter scaling, and the break time of an initially localized packet scales algebraically with the strength of disorder.

ACKNOWLEDGMENTS

We thank Dr. H Schomerus for fruitful discussions at the early stage of the present work. This work was sponsored partly by Grants No. NSF ECCS-1128571, No. DMR-1205223, No. ECCS-1128542, No. and DMR-1205307 and by AFOSR MURI Grant No. FA9550-14-1-0037.

[1] P. Anderson, Phys. Rev. **109**, 1492 (1958).
[2] D. S. Wiersma, P. Bartolini, Ad Lagendijk, and R. Righini, Nature (London) **390**, 671 (1997).
[3] A. A. Chabanov, M. Stoytchev, and A. Z. Genack, Nature (London) **404**, 850 (2000).
[4] M. Störzer, P. Gross, C. M. Aegerter, and G. Maret, Phys. Rev. Lett. **96**, 063904 (2006).
[5] J. D. Bodyfelt, M. C. Zheng, T. Kottos, U. Kuhl, and H. J. Stockmann, Phys. Rev. Lett. **102**, 253901 (2009).
[6] H. Hu, A. Strybulevych, J. H. Page, S. E. Skipetrov, and B. A. van Tiggelen, Nature (London) **4**, 945 (2008).
[7] H. Cao, Y. G. Zhao, S. T. Ho, E. W. Seelig, Q. H. Wang, and R. P. H. Chang, Phys. Rev. Lett. **82**, 2278 (1999); H. Cao, Waves Random Media **13**, R1 (2003).
[8] Y. Lahini, A. Avidan, F. Pozzi, M. Sorel, R. Morandotti, D. N. Christodoulides, and Y. Silberberg, Phys. Rev. Lett. **100**, 013906 (2008).
[9] T. Pertsch, U. Peschel, J. Kobelke, K. Schuster, H. Bartelt, S. Nolte, A. Tunnermann, and F. Lederer, Phys. Rev. Lett. **93**, 053901 (2004).
[10] T. Schwartz, G. Bartal, S. Fishman, and M. Segev, Nature (London) **446**, 52 (2007).

[11] J. Billy, V. Josse, Z. Zuo, A. Bernard, B. Hambrecht, P. Lugan, D. Clément, L. Sanchez-Palencia, P. Bouyer, and A. Aspect, Nature (London) **453**, 891 (2008).

[12] G. Roati, C. D'Errico, L. Fallani, M. Fattori, C. Fort, M. Zaccanti, G. Modugno, M. Modugno, and M. Inguscio, Nature (London) **453**, 895 (2008).

[13] J. C. J. Paasschens, T. Sh. Misirpashaev, and C. W. J. Beenakker, Phys. Rev. B **54**, 11887 (1996); C. W. J. Beenakker, J. C. J. Paasschens, and P. W. Brouwer, Phys. Rev. Lett. **76**, 1368 (1996); V. Freilikher, M. Pustilnik, and I. Yurkevich, Phys. Rev. B **50**, 6017 (1994).

[14] S. A. Ramakrishna, E. Krishna Das, G. V. Vijayagovindan, and N. Kumar, Phys. Rev. B **62**, 256 (2000); A. A. Asatryan, N. A. Nicorovici, P. A. Robinson, C. M. de Sterke, and R. C. McPhedran, *ibid.* **54**, 3916 (1996); A. A. Asatryan, N. A. Nicorovici, L. C. Botten, C. M. de Sterke, P. A. Robinson, and R. C. McPhedran, *ibid.* **57**, 13535 (1998); A. Sen, Indian J. Phys. **72A**, 363 (1998).

[15] X. Jiang, Q. Li, and C. M. Soukoulis, Phys. Rev. B **59**, R9007 (1999).

[16] D. N. Christodoulides, F. Lederer, and Y. Silberberg, Nature (London) **424**, 817 (2003).

[17] L. Martin, Opt. Express **19**, 13636 (2011); A. Szameit, *ibid.* **15**, 1579 (2007); A. W. Snyder and J. D. Love, *Optical Waveguide Theory* (Chapman and Hall, London, 1983).

[18] A. Guo, G. J. Salamo, D. Duchesne, R. Morandotti, M. Volatier-Ravat, V. Aimez, G. A. Siviloglou, and D. N. Christodoulides, Phys. Rev. Lett. **103**, 093902 (2009).

[19] T. Eichelkraut, R. Heilmann, S. Weimann, S. Stützer, F. Dreisow, D. N. Christodoulides, S. Nolte, and A. Szameit, Nat. Commun. **4**, 2533 (2013).

[20] C. E. Ruter, K. G. Makris, R. El-Ganainy, D. N. Christodoulides, M. Segev, and D. Kip, Nat. Phys. **6**, 192 (2010).

[21] A. V. Izyumov and B. D. Simons, Phys. Rev. Lett. **83**, 4373 (1999); Europhys. Lett. **45**, 290 (1999).

[22] P. G. Silvestrov, Phys. Rev. B **64**, 075114 (2001).

[23] A. Jazaeri and I. I. Satija, Phys. Rev. E **63**, 036222 (2001).

[24] A. E. Siegman, J. Opt. Soc. Am. A **20**, 1617 (2003).

[25] The reasoning for investigating ϕ_n at any frequency ω rather than at the eigenfrequencies is based on the Borland conjecture [26] which states that when ω is close to an eigenfrequency the exponential growth or decay of ϕ_n at distant sites converges to the exponential rate of amplitude variation of the corresponding eigenstate around its localization center.

[26] R. E. Borland, Proc. R. Soc. London, Ser. A **274**, 529 (1963).

[27] M. Kappus and F. Wegner, Z. Phys. B **45**, 15 (1981); B. Derrida and E. Gardner, J. Phys. (Paris) **45**, 1283 (1984).

[28] In the delocalized limit the wave functions of a perfect lattice are $\phi_n^{(k)} = \sqrt{\frac{2}{N+1}}\sin(\frac{nk\pi}{N+1})$ where $n,k = 1,\ldots,N$. Then the participation number, in the large-N limit, can be evaluated analytically to be $\xi_N \approx \frac{2}{3}N$.

[29] G. Casati, I. Guarneri, F. Izrailev, S. Fishman, and L. Molinari, J. Phys.: Condens. Matter **4**, 149 (1992).

[30] Y. V. Fyodorov and A. D. Mirlin, Phys. Rev. Lett. **69**, 1093 (1992).

[31] F. M. Izrailev, T. Kottos, and G. P. Tsironis, J. Phys.: Condens. Matter **8**, 2823 (1996); K. Frahm, A. Müller-Groeling, J.-L. Pichard, and D. Weinmann, in *Quantum Transport in Semiconductor Submicron Structures*, NATO ASI Series 326 (Kluwer Academic Publishers, Dordrecht/Boston/London, 1996), p. 173.

[32] The power-law behavior $\tilde{C}(z) \sim 1/z$ continues to hold also in the case of uniformly lossy or gain periodic waveguide arrays once the rescale with the norm Eq. (10) is taken into consideration.